THE JOURNAL OF BIOLOGICAL CHEMISTRY VOL. 281, NO. 41, pp. 31061–31069, October 13, 2006

Conformation of Amyloid Fibrils of β_2-Microglobulin Probed by Tryptophan Mutagenesis*[S]

Received for publication, June 5, 2006, and in revised form, July 17, 2006 Published, JBC Papers in Press, August 10, 2006, DOI 10.1074/jbc.M605358200

Miho Kihara[‡], Eri Chatani[‡1], Kentaro Iwata[‡], Kaori Yamamoto[‡], Takanori Matsuura[‡], Atsushi Nakagawa[‡], Hironobu Naiki[§], and Yuji Goto[‡2]

From the [‡]Institute for Protein Research, Osaka University, and CREST, Japan Science and Technology Agency, Yamadaoka 3-2, Suita, Osaka 565-0871, Japan and the [§]Department of Pathological Sciences, Faculty of Medical Sciences, University of Fukui and CREST, Japan Science and Technology Agency, Matsuoka, Fukui 910-1193, Japan

β_2-Microglobulin (β2-m), a protein responsible for dialysis-related amyloidosis, adopts an immunoglobulin domain fold in its native state. Although β2-m has Trp residues at positions 60 and 95, both are located near the surface of the domain. Hence, β2-m does not have a conserved Trp common to other immunoglobulin domains, which is buried in close proximity to the disulfide bond. To study the structure of amyloid fibrils in relation to their native fold, we prepared a series of Trp mutants. Trp^{60} and Trp^{95} were both replaced with Phe, and a single Trp was introduced at various positions. Among various mutants, W39-β2-m, in which a Trp was introduced at the position corresponding to the conserved Trp, exhibited a remarkable quenching of fluorescence in the native state, as observed for other immunoglobulin domains. An x-ray structural analysis revealed that W39-β2-m assumes the native fold with Trp^{39} located in the vicinity of the disulfide bond. Comparison of the fluorescence spectra of various mutants for the native and fibrillar forms indicated that, while the Trp residues introduced in the middle of the β2-m sequence tend to be buried in the fibrils, those located in the C-terminal region are more exposed. In addition, the fluorescence spectra of fibrils prepared at pH 2.5 and 7.0 revealed a large difference in the fluorescence intensity for W60-β2-m, implying a major structural difference between them.

Amyloidosis accompanies the deposition of normally soluble proteins into insoluble amyloid fibrils (1–3). Among various amyloidogenic proteins, β_2-microglobulin (β2-m)[3] is a target of extensive study because of its clinical importance and a suitable size for examining the relation between protein folding and amyloid fibril formation (4–11). β2-m, a typical immunoglobulin domain made of seven β-strands and one intramolecular disulfide bond (12, 13), is present as the non-polymorphic light chain of the class I major histocompatibility complex (14) (Fig. 1). As a part of its normal catabolic cycle, β2-m dissociated from the complex is transported in serum to the kidneys where the majority (95%) of it is degraded (15). Renal failure disrupts the clearance of β2-m from the serum and moreover β2-m does not pass through the dialysis membrane, resulting in an increase in the β2-m concentration by up to 50-fold in the blood circulation (15). When a high blood level is retained for more than 10 years, β2-m then self-associates to form amyloid fibrils, causing dialysis-related amyloidosis (15, 16).

The results so far obtained with various approaches suggest a picture of β2-m amyloid fibrils with an increased amount of β-structure in comparison with the native structure, including the transformation of native β-turns, but with disordered N- and C-terminal regions (6–9, 17). However, details remain unknown. To address the structure of amyloid fibrils, we have taken advantage of the unique properties of Trp fluorescence. One important feature of immunoglobulin domains is the presence of a buried Trp residue located close to the conserved disulfide bonds (18), leading to a strong quenching of Trp fluorescence (19, 20). We noticed that, although β2-m has two Trp residues (*i.e.* Trp^{60} and Trp^{95}), neither of these corresponds to the buried Trp common to other immunoglobulin domains. In the x-ray crystallographic structure of wild-type β2-m, while Trp^{60} located on the β-turn connecting β-strands D and E is exposed to solvent, Trp^{95} at the end of β-strand G is partially buried (Fig. 1). We designed and expressed a series of single Trp mutants in which Trp residues of wild-type β2-m have been deleted and a new Trp residue was introduced at various positions. Examination of the fluorescence spectra of mutants in the native and amyloid states revealed a notable conformational change upon the formation of amyloid fibrils.

EXPERIMENTAL PROCEDURES

β2-m Amyloid Fibril Formation—The expression and purification of human recombinant β2-m and the single Trp mutants were achieved as described previously (21). Acidic pH fibrils were prepared by a repeated seed-dependent extension with human recombinant β2-m expressed in *Escherichia coli* (21). or yeast *Pichia pastoris* (22). Neutral pH fibrils were prepared at pH 7.0 by a repeated seeding starting with the acidic pH fibrils

* This work was supported in part by the Takeda Science Foundation, and by Grants-in-Aid from the Japanese Ministry of Education, Culture, Sports, Science and Technology on Priority Areas (No. 40153770). The costs of publication of this article were defrayed in part by the payment of page charges. This article must therefore be hereby marked "*advertisement*" in accordance with 18 U.S.C. Section 1734 solely to indicate this fact.

[S] The on-line version of this article (available at http://www.jbc.org) contains supplemental Figs. S1–S3.

The atomic coordinates and structure factors (codes 2D4D and 2D4F) have been deposited in the Protein Data Bank, Research Collaboratory for Structural Bioinformatics, Rutgers University, New Brunswick, NJ (http://www.rcsb.org/).

[1] Recipient of a Japan Society for Promotion of Science (JSPS) postdoctoral fellowship.

[2] To whom correspondence should be addressed. Fax: 81-6-6879-8616; E-mail: ygoto@protein.osaka-u.ac.jp.

[3] The abbreviations used are: β2-m, β_2-microglobulin; AFM, atomic force microscopy; Gdn-HCl, guanidine hydrochloride; ThT, thioflavin T; λ_{max}, peak wavelength of Trp fluorescence; RMS, root mean square; PDB, Protein Data Bank; PEG, polyethylene glycol.

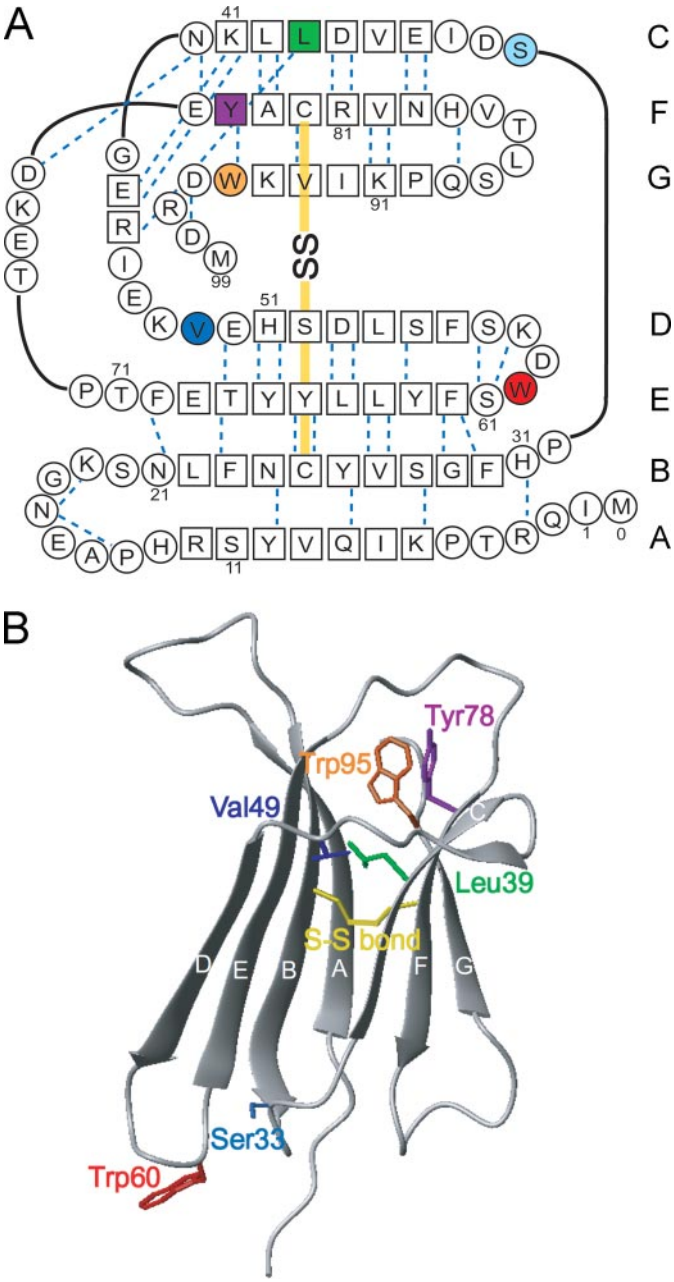

FIGURE 1. **Structure of β2-m and location of mutations introduced.** *A*, amino acid sequence. Trp[60] and Trp[95] are indicated in *red* and *orange*, respectively. Residues mutated to Trp are Leu[39] (*green*), Ser[33] (*cyan*), Val[49] (*blue*), and Tyr[78] (*purple*). A Met is always present at the N terminus of all the β2-ms, which is indicated as *M0*. *B*, schematic structure. Side chains of Trp[60] and Trp[95] and the residues mutated to Trp are indicated with the same colors as in *A*. Secondary structures are indicated by hydrogen bonds (*A*) and the numbering of β-strands (*A* and *B*). The schematic structure was produced using MOLMOL (43) with our structure (PDB code 2D4F).

(23). Throughout the experiments, we incubated the solutions for the formation of fibrils without agitation. The standard buffers used were 50 mM sodium citrate buffer (pH 2.5) containing 100 mM NaCl and 50 mM sodium phosphate buffer (pH 7.0) containing 100 mM NaCl. β2-m fibrils were originally purified from patients suffering from dialysis-related amyloidosis. Seeds (*i.e.* fragmented fibrils) were prepared by sonication of 200-μl aliquots of a fibril stock solution using a Microson sonicator (Misonix, Farmingdale, NY) as described previously (23). The fibril concentrations were measured with a Micro BCA™ Protein Assay Reagent kit (Pierce).

The amyloid extension reactions of mutant β2-ms were carried out using the wild-type neutral pH seeds and wild-type acidic pH seeds at pH 7.0 and 2.5, respectively. The extension reaction mixture at pH 2.5 contained 25 μM monomeric β2-m and 5 μg/ml acidic seeds. The extension reaction mixture at pH 7.0 contained 25 μM monomeric β2-m, 30 μg/ml neutral pH seeds, and 0.5 mM SDS (23). A low concentration of SDS, below its critical micelle concentration, is considered to stabilize the seeds and fibrils, to induce conformational change of monomers, and most importantly, to induce the oligomerization of β2-m. The reaction was monitored by the fluorometric assay with thioflavin T (ThT) at pH 8.5 as described previously (21–23).

AFM images were obtained using a Nano Scope IIIa (Digital Instruments) as described previously (24). The total internal reflection fluorescence microscopy system to observe ThT-bound amyloid fibrils was developed based on the use of an inverted microscope (IX70; Olympus, Tokyo, Japan) as described previously (25).

Trp Fluorescence Measurements—Trp fluorescence spectra were measured with a Hitachi F-4500 spectrofluorometer at 25 °C and a β2-m concentration of 0.05 mg/ml with excitation at 295 nm and monitored at 300–450 nm. Urea- or Gdn-HCl-dependent unfolding transitions of β2-m in the monomeric or amyloid state were measured using the change of Trp fluorescence. Before the measurements, the samples were incubated for 24 h at 25 °C. To compare the spectra of various single Trp β2-m mutants in the native or fibrillar state, the spectra of the unfolded states in 5.5 M Gdn-HCl or 10 M urea are assumed to be the same independent of mutations. We did not normalize the spectra of the unfolded states under different conditions. The spectra of wild-type β2-m with two Trp residues in 5.5 M Gdn-HCl or 10 M urea are assumed to have an intensity 2-fold those of single Trp mutants. We consider that this normalization provides a more accurate comparison of the spectra of various mutants particularly for amyloid fibrils.

A Two-state Unfolding Transition Analysis of the Native State—For the unfolding of the native state at pH 8.0, we further analyzed the results assuming a two-state transition between the native and denatured states (21). To obtain the fraction of unfolded species (f_U), the fluorescence spectra from 310 nm to 450 nm were fitted to Equation 1,

$$F = \alpha\{f_U F_U + (1 - f_U)F_N\} \quad \text{(Eq. 1)}$$

where F is the spectrum for a sample with each concentration of denaturant, F_N and F_D that for without denaturant and the highest concentration of denaturant, respectively, f_U is the fractional population of unfolded species, and α is a variable term for fluorescence intensity (21). Exceptionally, for the monomeric states of W39- and W33-β2-m,[4] which did not show a change in maximal wavelength but exhibited a significant change in intensity upon unfolding (see

[4] W33-, W39-, W49-, W60-, W78-, and W95-β2-ms: single Trp mutants with a single Trp at the indicated residue number, where W60- and W95-β2-ms contain W95F and W60F mutations, respectively, and W33-, W39-, W49-, and W78-β2-ms contain triple mutations of W60F/W95F/S33W, W60F/W95F/L39W, W60F/W95F/V49W, and W60F/W95F/Y78W respectively.

"Results"), spectral area was calculated at each concentration of Gdn-HCl and used for the determination of f_U. f_U was plotted against the concentration of denaturant. The free energy change of unfolding (ΔG_U) was calculated by a least-squares fitting shown in Equation 2,

$$f_U(y) = 1/\{1 + \exp(-\Delta G_U/RT)\} \quad \text{(Eq. 2)}$$

where $f_U(y)$ is the observed f_U, R is the gas constant and T is temperature. Then, a standard linear relation was assumed between ΔG_U and the concentration of denaturant[denaturant]) in Equation 3,

$$\Delta G_U = \Delta G_{U,H20} - m[\text{denaturant}] \quad \text{(Eq. 3)}$$

where $\Delta G_{U,H20}$ is ΔG_U in water and m is a measure for cooperativity of unfolding. The midpoint concentration of unfolding, C_m, is calculated in Equation 4.

$$C_m = \Delta G_{U,H20}/m \quad \text{(Eq. 4)}$$

X-ray Crystallographic Analysis—Crystals of the monomeric wild-type and W39-β2-ms were grown by the hanging-drop vapor diffusion method (26). For wild-type β2-m, the reservoir solution contained 20% (w/v) PEG 4000, 25% (v/v) glycerol, 200 mM ammonium acetate, and 100 mM sodium acetate at pH 5.6. The reservoir solution for W39-β2-m contained 15% (w/v) PEG 4000, 25% (v/v) glycerol, 200 mM ammonium acetate, and 100 mM sodium acetate at pH 5.6. Crystal-growth droplets (3 μl) were composed of 2 μl of protein solution at 8–12 mg ml^{-1} and 4–5 mg ml^{-1} for wild-type and W39-β2-m, respectively, in 25 mM sodium acetate at pH 5.6 and 1 μl of reservoir solution, and were incubated at 15 °C.

X-ray diffraction data were collected to a resolution of 1.7 Å for wild-type β2-m and 2.1 Å for W39-β2-m on a R-AXIS VII image plate detector, using graphite-monochromated CuK$_\alpha$ radiation (1.5418 Å generated from an FR-E Super-Bright rotating anode operated at 45 kV and 45 mA) (Rigaku, Japan). Diffraction images were indexed and integrated with MOSFLM software (27), and then scaled and merged with the SCALA program (CCP4) (28). To solve the structures, the molecular replacement program MOLREP (29) was used on the basis of the monomeric structure (Protein Data Bank ID code 1LDS) reported previously (12). The model was built with the program O (30) and refined using REFMAC5 (31). Progress with the refinement was

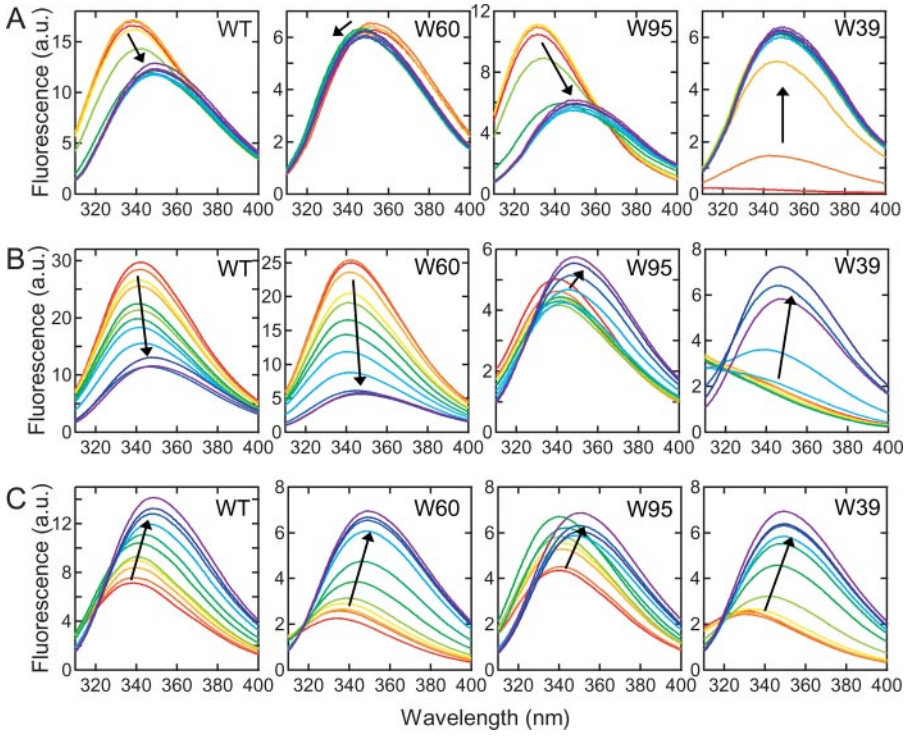

FIGURE 2. **Unfolding transitions of the native state and amyloid fibrils of various β2-m mutants.** Unfolding transitions were monitored by Trp fluorescence spectrum of wild-type β2-m and single Trp β2-m mutants (W60, W95, and W39) in the monomeric state at pH 8.0 (*A*) and in the amyloid fibrils at pH 2.5 (*B*) and pH 7.0 (*C*). *A* and *B*, concentration of Gdn-HCl increases from 0 M (*red*) to 5.5 M (*purple*) in steps of 0.5 M, as guided by an *arrow*. *C*, concentration of urea increases from 0 M (*red*) to 10.0 M (*purple*) in steps of 1.0 M, as guided by an *arrow*.

TABLE 1
Comparison of conformation and stability of the wild-type and single Trp β2-ms

Protein	Monomers at pH 7.0							Fibrils at pH 2.5				Fibrils at pH 7.0			
	$\Delta G_{U,H20}$[a]	m[a]	C_m[b]	R[c]	Q[d]	λ_N[e]	λ_D[e]	C_m[b]	Q[d]	λ_f[e]	λ_D[e]	C_m[b]	Q[d]	λ_f[e]	λ_D[e]
	kJ mol^{-1}	kJ mol^{-1} M^{-1}	M	Å	%	nm	nm	M	%	nm	nm	M	%	nm	nm
Wild type	22.4	10.2	2.2		200	337	350	4.1	200	342	347	6.4	200	339	349
W60				19.5	81	353	350	4.4	167	342	347	5.8	62	333	348
W95	25.5	11.1	2.3	9.3	106	331	348	3.6	35	342	348	6.5	124	339	351
W39	9.2	13.1	0.7	6.8	3		348	4.2	17		347	4.8	69	331	350
W33	18.0	12.0	1.5	14.6	107	349	350	4.7	27	337	350				
W49				11.6	66	344	349	4.2	11		348	4.9	72	338	349
W78	15.8	8.8	1.8	10.5	78	325	349	4.2	8		348	6.4	47	338	349

[a] The free energy change of unfolding in the absence of denaturant ($\Delta G_{U,H20}$) and a measure for cooperativity of unfolding (m) as described by Equation 3.
[b] Midpoint denaturant concentration of unfolding.
[c] Distance between the Cα of the Trp residue and the center of the Cys^{25}–Cys^{80} disulfide bond, which was calculated from the coordinate of wild-type β2-m (PDB ID code 2D4F).
[d] Relative fluorescence spectral area of Trp among various mutants in the same conformational states where those of the wild-type β2-m with two Trp residues were defined to be 200%.
[e] Maximal wavelength of Trp fluorescence in the native state (λ_N), denatured state (λ_D), or amyloid fibrils (λ_f).

monitored by comparing the *R* factor to the free *R* factor (32). The geometry of the model was monitored using the program PROCHECK (33), the Ramachandran plot showing that 99% of the residues lie in the allowed region.

RESULTS

CD Spectra of Single Trp Mutants—CD spectra of single Trp β2-ms were measured at pH 8.0 (see supplemental Fig. S1). The far-UV CD spectra of all the mutants were similar to those of wild-type β2-m (23). On the other hand, the near-UV CD spectra were differed, indicating that Trp residues contribute to the near-UV CD and that the environment of these residues differs depending on the mutant. Thus, in overall structure, the single Trp mutants were similar to the wild type.

Trp Fluorescence Spectra of Single Trp Mutants—We characterized the single Trp mutants using Trp fluorescence (Fig. 2, Table 1, see also supplemental Fig. S2). The fluorescence spectrum of wild-type β2-m in the native state at pH 8.0 showed a maximum (λ_{max}) at 337 nm (Fig. 2*A*). The addition of high concentrations of Gdn-HCl resulted in a red shift of the λ_{max} to 350 nm, accompanied by a decrease in the intensity of fluorescence. W60-β2-m showed a λ_{max} at 353 nm even in the absence of Gdn-HCl and an increase in the Gdn-HCl concentration resulted in only a slight shift of the λ_{max} to a shorter wavelength accompanied by a slight decrease in fluorescence (Fig. 2*A*). The results are consistent with the complete exposure of Trp^{60} in the crystallographic structure (12). On the other hand, the fluorescence spectrum of W95-β2-m showed a similar change to that of the wild type, indicating that, although Trp^{95} is partly buried, it is not quenched by the disulfide bond (Fig. 2*A*). In fact, the fluorescence spectrum of wild-type β2-m was reproduced by adding the spectra of W60- and W95-β2-ms (Fig. 3*A*, *dashed line*). These results clearly demonstrate that Trp^{95} predominantly contributes to the fluorescence of wild-type β2-m.

W39-β2-m is a triple mutant in which Trp^{60} and Trp^{95} were replaced by Phe, and Leu^{39}, the position of the conserved Trp residue common to many immunoglobulin domains, was replaced by Trp. The fluorescence spectrum of W39-β2-m exhibited complete quenching in the absence of Gdn-HCl (Fig. 2*A*). These observations are consistent with an immunoglobulin domain having a Trp residue at the corresponding position (19, 20), in which the fluorescence of the conserved Trp is quenched by the disulfide bond. A cooperative change in fluorescence intensity was observed with an increase in the concentration of Gdn-HCl, suggesting that W39-β2-m assumes the native fold in the absence of Gdn-HCl (see below).

Other mutants studied were W33-, W49-, and W78-β2-ms (Fig. 3*A*, see supplemental Fig. S2). With an increase in the Gdn-HCl concentration, the fluorescence of W33-β2-m showed no shift in λ_{max}, and the intensity decreased slightly, indicating that Trp^{33} is exposed. The Trp fluorescence of W49-β2-m showed a slight shift in the λ_{max} toward a longer wavelength and a slight increase in intensity, indicating that Trp^{49} is partly buried and slightly quenched. The Gdn-HCl-induced spectral change of W78-β2-m was similar to that of wild-type β2-m, although the λ_{max} of the native state was shorter than that of the wild type. The result indicates that Trp^{78} of W78-β2-m is more buried than Trp^{95} of the wild type.

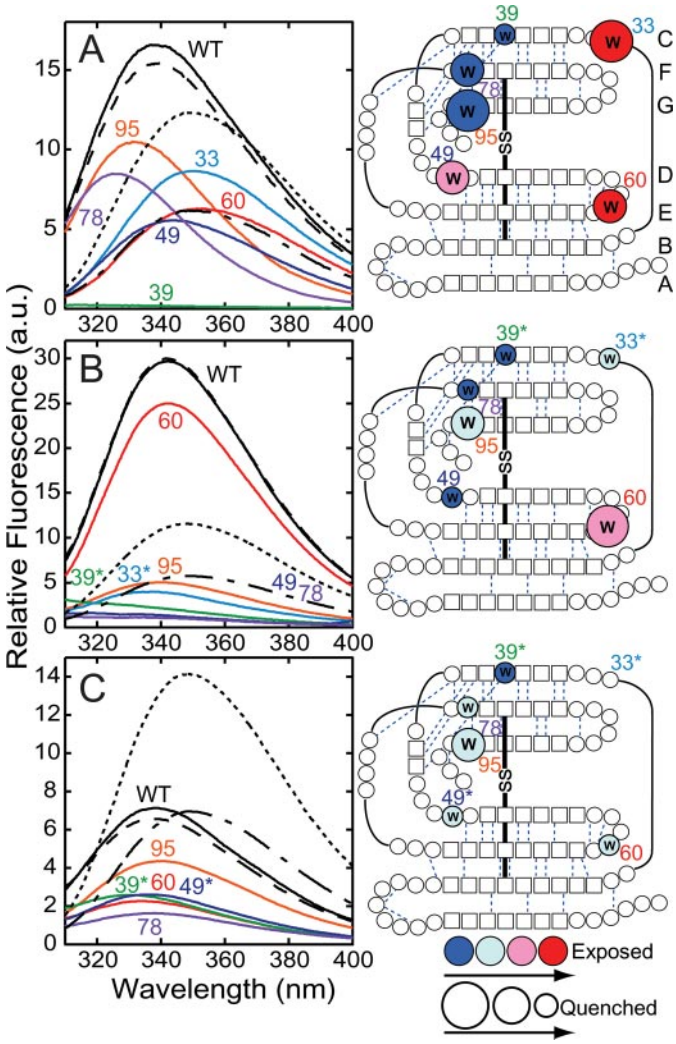

FIGURE 3. **Comparison of Trp fluorescence spectra of the native state and amyloid fibrils of various β2-m mutants.** *A*, monomeric β2-m Trp mutants at pH 8.0. *B* and *C*, amyloid fibrils at pH 2.5 (*B*) and pH 7.0 (*C*). The spectra of wild-type β2-m and W39-β2-m, as an example of the mutants, in 5.5 M Gdn-HCl at pH 8.0 (*A*) or pH 2.5 (*B*), or in 10 M urea at pH 7.0 (*C*) are also shown with *dotted lines* and *dash-dot lines*, respectively. The locations of Trp residues in mutants are indicated by residue number. Under the respective conditions, the spectra were normalized assuming that the maximal fluorescence intensity of each single Trp mutant in the unfolded state is the same, and half that of wild-type β2-m with two Trp residues. Simulated spectra (*dashed lines*) of wild-type β2-m assuming the sum of those of W60- and W95-β2-ms are indicated. Diagrams to the *right* show the extents of burial of Trp side chain and fluorescence quenching observed for each mutant, mapped on the secondary structures of native β2-m. The thresholds for the degree of burial are *blue*, $\lambda_{max} < 330$ nm; *right blue*, 330 nm $< \lambda_{max} <$ 340 nm; *pink*, 340 nm $< \lambda_{max} <$ 345 nm; and *red*, 345 nm $< \lambda_{max}$. The degree of quenching, considering λ_{max} and fluorescence intensity, is represented by the *circles* in three sizes. *Asterisks* for the labels of W33- and W39-β2-ms at pH 2.5 and W33-, W39-, and W49-β2-ms at pH 7.0 indicate the altered kinetics of fibril formation or no fibril formation (*i.e.* W33 at pH 7.0).

Altogether, the fluorescence spectra of the single Trp mutants are consistent with the location of mutated residues in the x-ray native structure (Fig. 1), arguing that these mutants provide excellent probes with which to monitor the conformational change upon the formation of fibrils.

The Gdn-HCl-induced unfolding transitions were constructed on the basis of the spectral change (Fig. 4). In the cases

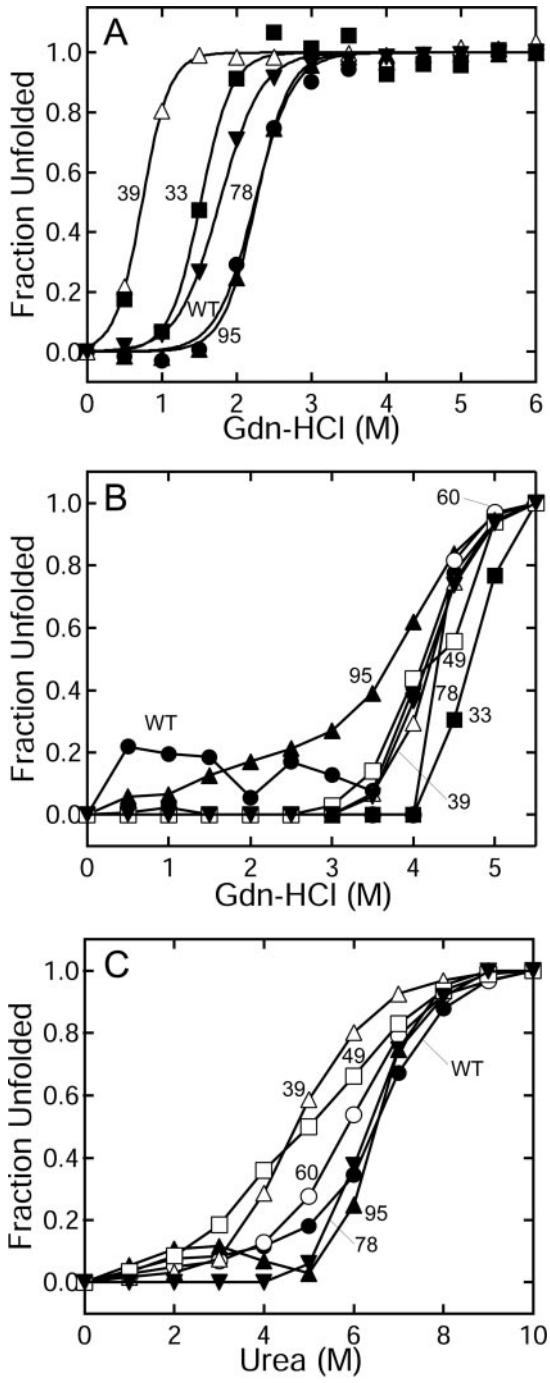

FIGURE 4. **Stability of monomeric β2-m Trp mutants at pH 8. 0 (*A*) and their amyloid fibrils at pH 2.5 (*B*) and pH 7.0 (*C*) at 25 °C.** Stability was assessed by measuring Trp fluorescence and the fraction unfolded was obtained assuming a two-state transition between the native and unfolded states (*A*) or the fibrillar and unfolded states (*B* and *C*). For the monomers, the normalized transition curve was further analyzed to obtain the theoretical curve as indicated. Proteins are wild-type (●), W60 (○), W95 (▲), W39 (△), W33 (■), W49 (□), and W78 (▼) β2-ms.

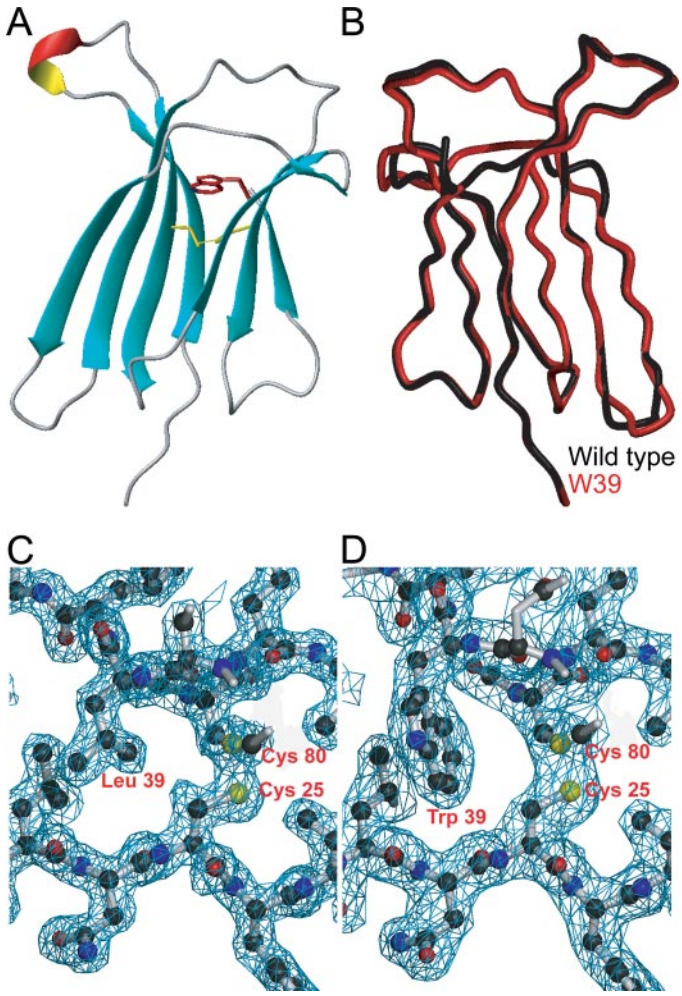

FIGURE 5. **X-ray crystallographic analysis of wild-type and W39-β2-ms.** *A*, ribbon model of the determined structure of W39-β2-m (PDB ID code 2D4D). The introduced Trp[39] residue and disulfide bond are indicated by stick models colored in *red* and *yellow*, respectively. *B*, superimposition of the main chains of wild-type (*black*) and W39 (*red*) β2-ms, which was performed with atoms belonging to β-strands. *C* and *D*, $2F_o - F_c$ maps for wild-type (*C*) and W39 (*D*) β2-ms in the vicinity of residue 39. Electron densities are indicated by *cyan meshes*. The coordinates of carbon, sulfur, nitrogen, and oxygen atoms in the determined β2-m structures are indicated by *black*, *yellow*, *blue*, and *red balls*, respectively.

of W49- and W60-β2-ms, we could not obtain a transition curve because the location of the Trp residues on the surface resulted in no significant spectral change upon unfolding. For other mutants, it has been revealed that the stability decreased to various extents in comparison with that of the wild type. In particular, the destabilization was significant for W39-β2-m. It is conceivable that the replacement of Leu[39] located in the tightly packed interior of β2-m by bulky Trp induced significant steric hindrance. Thus, it is important to confirm the native fold of W39-β2-m.

X-ray Crystallographic Structures—We determined the crystallographic structures of wild-type and W39-β2-ms (Fig. 5) using the molecular replacement method on the basis of the monomeric crystal structure prepared at pH 5.7 (12). Both crystals belong to space group C2 and the unit cell dimensions are $a = 77.6$ Å, $b = 28.8$ Å, $c = 54.8$ Å, and $\beta = 121.7°$ for the wild-type and $a = 77.4$ Å, $b = 28.8$ Å, $c = 57.2$ Å, and $\beta = 123.6°$ for W39-β2-m. A summary of the refinement statistics is given in Table 2. The coordinates and structure factor amplitudes have been deposited in the Protein Data Bank (ID code 2D4F for the wild-type and 2D4D for W39-β2-m). Our structure of wild-type β2-m at pH 5.6 without a bulge in the βD strand is basically the same as that previously reported (12).

Despite the triple mutations (W60F/W95F/L39W), the crystal structure of W39-β2-m was very similar to that of wild-type

TABLE 2
Crystallographic data collection and refinement statistics

Crystal	Wild type	W39
Space group	C2	C2
Unit cell		
a	77.6	77.4
b	28.9	28.8
c	54.8	57.2
β	121.7	123.6
Resolution	38.0-1.7 (1.79-1.70)[a]	47.67-2.1 (2.21-2.20)[a]
Number of observed reflections	39670 (4129)[a]	22387 (3270)[a]
Number of unique reflections	11279 (1454)[a]	6343 (927)[a]
Completeness (%)	97.3 (87.1)[a]	100 (100)[a]
I/s (I)	8.1 (1.8)[a]	8.2 (2.4)[a]
R factor (%)	20.8	21.6
R free (%)	23.3	26.5
Number of protein atoms	918	857
Number of water molecules	72	48
Average overall B factor (Å)	18.42	26.44
RMS deviation ideal stereochemistry		
Bond length (Å)	0.013	0.010
Bond angle (degree)	1.45	1.30

[a] Values in parentheses are for the highest resolution shell.

β2-m (Fig. 5). The RMS deviations between them are 0.51 Å using main chain atoms, N, Cα, C, and O. Slight differences exist at residues Arg^{45}-His^{51} on the CD loop and Lys^{58}-Trp^{60} on the DE loop. The difference in the CD loop is caused by a difference in crystal packing interactions with symmetry-related β2-m molecules. For the DE loop, the mutation of Trp to Phe should yield a void, possibly producing the deviation. The structure of W39-β2-m shows tight contact between Trp^{39} and the disulfide bond, with the aromatic ring plane facing the disulfide bond in parallel as observed for other immunoglobulin domains (Fig. 5*D*) (18). The results reveal the native fold of W39-β2-m and furthermore the proximity of Trp^{39} to the disulfide bond, proposing the structural basis for the complete quenching of Trp fluorescence. Moreover, a clear calorimetric peak typical of the unfolding of globular proteins was observed for W39-β2, although decreases in stability were also evident (see supplemental Fig. S3). Additionally, W49- and W60-β2-ms, whose conformational stability could not be evaluated based on Trp spectral change, also exhibited calorimetric peaks, supporting the native fold of these mutants.

Formation of Amyloid Fibrils—The formation of amyloid fibrils of single Trp mutants was studied using seed-dependent extension at pH 2.5 and 7.0, and monitored by measuring ThT fluorescence (Fig. 6). At each pH, seed fibrils prepared with wild-type β2-m were used, ensuring the formation of fibrils with wild-type structures even when various amyloid conformations can coexist (23, 34). At pH 2.5, most of the mutants except W33- and W49-β2-ms completed the extension reaction in a couple of hours, similar to the standard kinetics of fibril growth with wild-type β2-m (21, 24). W33- and W49-β2-ms showed a lag-phase. Because we used the wild-type seeds, it is possible that the lag-phase represents the difficulty of accommodating these bulky mutations at Ser^{33} and Val^{49}, producing a slightly different type of fibrils. The final intensity of ThT depended on the mutant, suggesting that the exact structure of

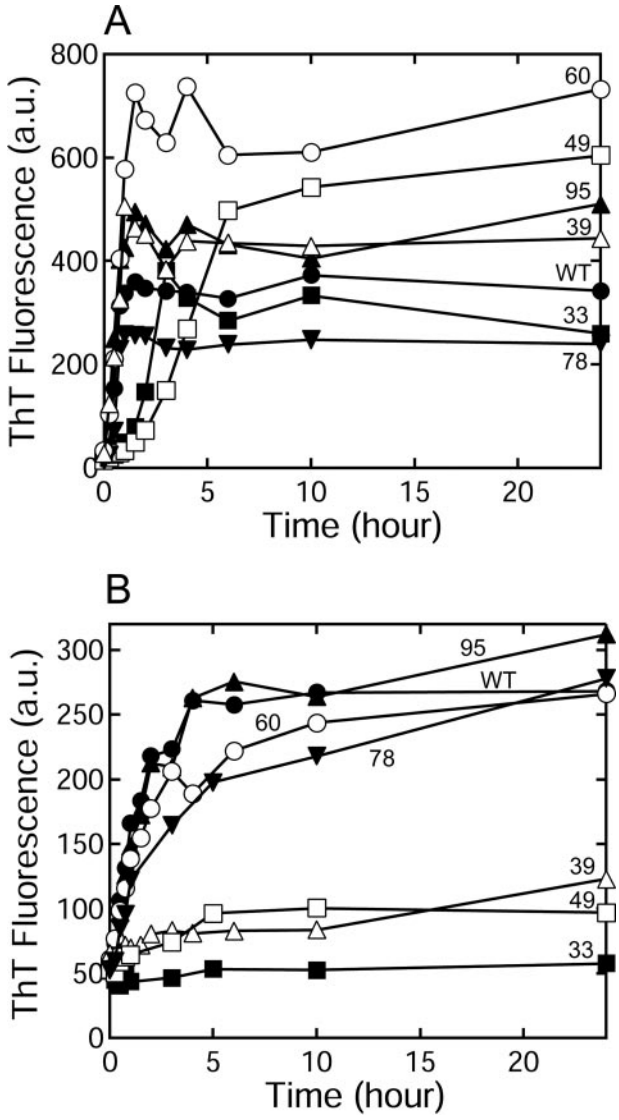

FIGURE 6. **Formation of amyloid fibrils of single Trp β2-m mutants.** Seeding-dependent fibril growth at pH 2.5 (*A*) and pH 7.0 (*B*) at 37 °C monitored by fluorometric assay with ThT. Proteins are wild-type (●), W60 (○), W95 (▲), W39 (△), W33 (■), W49 (□), and W78 (▼) β2-ms.

the amyloid fibrils depends on the site of mutation, as previously discussed (21).

At pH 7.0, wild-type β2-m exhibits seed-dependent fibril extension in the presence of maturated seeds and 0.5 mM SDS, although several hours are required, and the final level of ThT fluorescence is less than that at pH 2.5 (23). At this stage of our experiments, 0.5 mM SDS was essential (23, 35). W60-, W95- and W78-β2-ms showed similar extension kinetics to wild-type β2-m. On the other hand, the formation of fibrils by W33-, W39- and W49-β2-ms was suppressed and enough amounts of fibrils for the subsequent experiments were not obtained for W33-β2-m. As was the lag-phase at pH 2.5, the significant suppressions may represent the difficulty of accommodating the bulky Trp mutations at Ser^{33}, Leu^{39}, and Val^{49} (Fig. 6*B*).

Fibrils of W39-β2-m as well as those of wild-type β2-m were confirmed to have formed at pH 2.5 and 7.0 by AFM (Fig. 7, *A–D*). Fibrils of W39-β2-m were also visualized with total internal reflection fluorescence microscopy taking advantage of

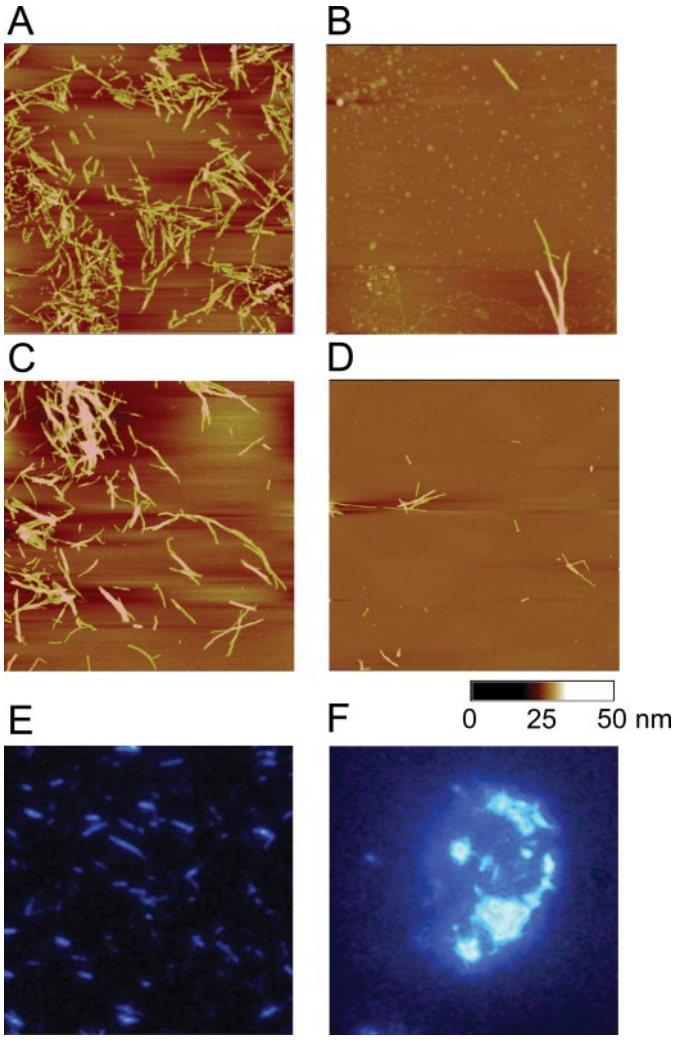

FIGURE 7. **AFM and total internal reflection fluorescence microscopic images of amyloid fibrils.** *A–D,* AFM images of amyloid fibrils of wild-type β2-m (*A* and *B*) and W39-β2-m (*C* and *D*) prepared at pH 2.5 (*A* and *C*) or pH 7.0 (*B* and *D*). *E* and *F*, total internal reflection fluorescence microscopic images of W39-β2-m prepared at pH 2.5 (*E*) or pH 7.0 (*F*). The side of an AFM image is 5-μm long and that of a fluorescence micrograph is 20 μm.

ThT fluorescence (Fig. 7, *E* and *F*). When measured by AFM, those that formed at pH 2.5 had a morphology typical of β2-m amyloid fibrils with a diameter of about 5–8 nm and a length of more than 1 μm as reported previously (36). Although the AFM of the fibrils prepared at pH 7.0 was more difficult as previously reported (24), we could detect some fibrils of wild-type β2-m and W39-β2-m. We previously confirmed that the fibrils of various β2-m mutants formed at pH 2.5 by electron microscopy (21). Therefore, in the present article, although we did not measure the AFM micrographs of fibrils of other Trp mutants, we believe that other mutants, except W33-β2-m at pH 7.0, also formed amyloid fibrils with an overall morphology similar to that of wild-type β2-m. However, for fibrils with Trp residue newly introduced, their exact structures might be slightly different from that of wild-type fibrils by the steric hindrance of Trp residue and other effects introduced by mutations.

Fluorescence Spectra of Amyloid Fibrils at pH 2.5—The amyloid fibrils of wild-type β2-m at pH 2.5 showed a λ_{max} at 342 nm (Fig. 2*B* and Table 1). Importantly, this λ_{max} is slightly longer than that of the monomeric native conformation at pH 7.0. As the Gdn-HCl concentration increased, the λ_{max} shifted to 347 nm accompanied by a marked decrease in intensity. The fluorescence intensity of the fibrils relative to the unfolded form in 5.5 M Gdn-HCl is much larger than that of the native structure at pH 7.0, implying an increased distance between the Trp residues and the disulfide bond.

The Gdn-HCl-dependent spectral change of W60-β2-m in the fibrils was similar to that of wild-type β2-m, although the relative change of fluorescence was larger than that of the wild type (Fig. 2*B*). In contrast, W95-β2-m in fibrils showed a moderately quenched spectrum with a λ_{max} at 342 nm and, upon unfolding, the fluorescence intensity increased accompanied by a red shift to 348 nm (Fig. 2*B*). Thus, the change in fluorescence upon the unfolding of the wild-type fibrils at pH 2.5 is mostly attributed to Trp^{60}, the opposite to the situation in the native state. The fluorescence spectrum of wild-type β2-m in the fibrils was reproduced exactly by summing those of W60- and W95-β2-ms (Fig. 3*B*, *dashed line*).

Regarding other mutants at pH 2.5, the fluorescence spectrum of W33-β2-m in fibrils was similar to that of W95-β2-m, suggesting that Trp residues of these mutants are buried and quenched to a similar extent (Fig. 3*B*, Table 1, and supplemental Fig. S2). In a marked contrast, the fluorescence of either W39-, W49-, or W78-β2-ms in the fibrils was strongly quenched and it was difficult to accurately estimate λ_{max}, suggesting that they are buried and are probably located close to the disulfide bond (Fig. 3*B*).

Fluorescence Spectra of Amyloid Fibrils at pH 7.0—The wild-type β2-m fibrils prepared at pH 7.0 showed a maximum at 339 nm (Fig. 2*C* and Table 1). Again, this maximum wavelength is slightly longer than that in the monomeric native state, suggesting more exposed Trp residues on average. Because the presence of 0.5 mM SDS caused precipitation of Gdn-HCl, we used urea as a denaturant. As the urea concentration increased, the fluorescence increased with a shift of λ_{max} to 349 nm. It is noted that the change in intensity is the opposite to that of the fibrils at pH 2.5.

The Gdn-HCl-induced change in fluorescence of W60-β2-m fibrils at pH 7.0 was similar to that of the wild type (Fig. 2*C*). On the other hand, the increase in the fluorescence of the W95-β2-m fibrils was moderate, indicating that Trp^{60} dominantly contributes to the observed increase in fluorescence of the wild-type β2-m at pH 7.0. The fluorescence spectrum of the wild type was the sum of the spectra of W60- and W95-β2-ms (Fig. 3*C*, *dashed line*). Thus, the large difference in the wild-type fibrils at pH 2.5 (Fig. 3*B*) and 7.0 (Fig. 3*C*) represents that, while Trp^{60} in the fibrils at pH 2.5 is slightly buried but not quenched, that at pH 7.0 is buried more and significantly quenched.

For other single Trp mutants, W39-β2-m showed a maximum at 331 nm (Fig. 2*C*, Table 1, supplemental Fig. S2). This wavelength was the shortest among the fibrils of the single Trp mutants, suggesting that Trp^{39} is most deeply buried in the fibrils at pH 7.0. The fluorescence spectra of the W49- and W78-β2-m fibrils were similar to the spectrum of the W60-β2-m fibrils (Fig. 2*C*). However, the quenching of the W39-, W49- and W78-β2-m fibrils was less extensive at pH 7.0 than at pH 2.5.

Unfolding Transitions of Amyloid Fibrils—To further address the mutational effects, the unfolding transition curves of the

fibrils against the concentration of Gdn-HCl at pH 2.5 and urea at pH 7.0 were constructed (Fig. 4, *B* and *C* and Table 1). Considering the complication of reversibility of fibril unfolding (37), the curves obtained after similar incubation periods give apparent transitions with which to compare the overall stability of fibrils. The fibrils exhibited cooperative unfolding transitions at both pH 2.5 and 7.0. The variation in the transition curves was not correlated with that in the native state at pH 7.0 (Fig. 4*A*). Intriguingly, the most unstable fibrils at pH 7.0 (W39- and W49-β2-ms) showed decreased amyloidogenicity at pH 7.0 (Figs. 4*C* and 6*B*).

DISCUSSION

Fluorescence Spectra in the Native State—Trp fluorescence is one of the most popular probes with which to study the conformation of proteins and peptides. By observing the λ_{max}, one can estimate whether Trp is in a polar environment exposed to water or in a non-polar environment buried in the polypeptide chain. Although the intensity of fluorescence increases with a decrease in polarity, various quenchers, most importantly the disulfide bond located close by, decreases the intensity (38). However, interpreting the spectra of fluorescence is not always straightforward since the presence of multiple Trp residues averages the respective contributions. Moreover, Trp is not so frequent among 20 amino acid residues, restricting the site of the conformational probe. In the present study, to take advantage of Trp fluorescence while excluding its disadvantages, a variety of single Trp mutants of β2-ms were prepared.

The x-ray crystallographic analysis demonstrated that even W39-β2-m, the most destabilized mutant, assumes the native structure (Fig. 5). The introduced Trp is located close to the disulfide bond as observed for other immunoglobulin domains (18), explaining the remarkable quenching of fluorescence. For other single Trp mutants, the variation in the spectra of fluorescence is exactly consistent with the location of substituted residues in the native structure (Fig. 1). The results argue that a series of single Trp mutants are indeed promising tools with which to probe the protein conformation.

Fluorescence Spectra in the Amyloid Fibrils—Most importantly, at both pH 2.5 and 7.0, the fluorescence spectrum of wild-type β2-m in the fibrils was reproduced exactly by summing those of W60- and W95-β2-ms (Fig. 3, *B* and *C*, *dashed lines*). This shows that W60- and W95-β2-ms form the amyloid fibrils similar to those of wild-type β2-m, validating the present approach to address the structure of amyloid fibrils. We consider that the fibrils of other mutants are also similar to those of wild-type β2-m in morphology and overall structure, even if not the same (21). However, presence of a lag-phase for W33- and W49-β2-ms at pH 2.5 and significant suppression for W33-, W39-, and W49-β2-ms at pH 7.0 suggests that the wild-type seeds do not easily accommodate these bulky mutations, leading to the formation of amyloid fibrils with altered local structures (Fig. 6). This interpretation is consistent with the observation that Ser^{33}, Leu^{39}, and Val^{49} are involved in the core of amyloid fibrils at pH 2.5 (17, 21) and that most unstable fibrils at pH 7.0 are those of W39- and W49-β2-ms. In other words, adequate packing of these residues is important for the fibril formation. Thus, Trp mutagenesis is also useful for probing the internal packing of amyloid fibrils.

The fluorescence spectra of amyloid fibrils were markedly different from those of the native conformation, providing important insights into the conformational differences between the two (Fig. 3). In the amyloid state at pH 2.5, Trp fluorescence of all the mutants except W60-β2-m was highly quenched, indicating these residues are located near quenchers, most importantly the disulfide bond. Interestingly, Trp^{39} was not completely quenched in the fibrils, suggesting a disruption of the tight contact between Trp^{39} and the disulfide bond in the native structure. Except W95-β2-m, the λ_{max} values are smaller in the fibrils than in the native state, suggesting that the Trp residues are more buried in the fibrils. Taken together, although Trp^{60} exposed on the native structure is buried upon the formation of a fibril, it is located relatively far from the disulfide bond. Trp^{95} is relatively buried in the native structure, while it is more exposed to the solvent in the fibrils, consistent with the idea that N and C-terminal regions are more exposed in the fibrils (6–9, 17).

Importantly, the present results suggest the structural basis of the polymorphism of β2-m amyloid fibrils (23, 39) and, furthermore, fibrils of other proteins (40–42). The fluorescence spectra of the amyloid forms at pH 7.0 are similar to those at pH 2.5, except for W60-β2-m (Figs. 2 and 3). While the fluorescence of W60-β2-m fibrils at pH 2.5 was significantly intense, it was quenched at pH 7.0 as for other mutants, suggesting the distance between Trp^{60} and the disulfide bond to be closer at pH 7.0. It is conceivable that the two types of fibrils can be distinguished in terms of the geometry between the DE loop on which Trp^{60} resides and the disulfide bond.

Finally, although the architecture of amyloid fibrils is still controversial, the most common model is that of several protofibrils associated laterally and that a single protofibril consists of a large number of monomers associated in tandem by cross-β sheet interactions (1–3). Consequently, when one considers burial and quenching using the Trp fluorescence, it is inevitable to consider the effects from other molecules in the same protofibril, and furthermore, from molecules in other protofibrils. The order of effects is likely to be: first the intramolecular interactions, second the intermolecular interactions in the protofilament, and then the intermolecular interactions between protofibrils. Therefore, although further studies distinguishing the different interactions and moreover additional evidence validating the present observations are essential, we believe that a series of residue-specific information obtained here will be useful to construct the overall images of amyloid fibrils as summarized below.

CONCLUSIONS

For most of the single Trp mutants, we observed signal changes indicating a significant conformational change between the native structure and amyloid fibrils. This suggests that the formation of amyloid fibrils of β2-m accompanies a significant conformational change to the entire molecule. Notable suppression of fibril formation at pH 7.0 observed for W33-, W39-, and W49-β2-ms suggests that the corresponding residues (*i.e.* Ser^{33}, Leu^{39}, and Val^{49}) are tightly packed in the wild-type fibrils, requiring local

conformational change for accommodating bulky Trp residues. The fibrils prepared at pH 2.5 and pH 7.0 exhibited a marked change in Trp^{60} fluorescence suggesting the structural basis of the polymorphism of β2-m amyloid fibrils (23, 39). Thus, mutagenesis of Trp would be a promising tool with which to probe the mechanism by which amyloid fibrils form.

Acknowledgment—We thank Dr. Tadato Ban for help with the total internal reflection fluorescence microscopy measurements.

REFERENCES

1. Rochet, J. C., and Lansbury, P. T., Jr. (2000) *Curr. Opin. Struct. Biol.* **10,** 60–68
2. Dobson, C. M. (2003) *Nature* **426,** 884–890
3. Uversky, V. N., and Fink, A. L. (2004) *Biochim. Biophys. Acta* **1698,** 131–153
4. Naiki, H., Hashimoto, N., Suzuki, S., Kimura, H., Nakakuki, K., and Gejyo, F. (1997) *Amyloid* **4,** 223–232
5. Kad, N. M., Myers, S. L., Smith, D. P., Smith, D. A., Radford, S. E., and Thomson, N. H. (2003) *J. Mol. Biol.* **330,** 785–797
6. McParland, V. J., Kalverda, A. P., Homans, S. W., and Radford, S. E. (2002) *Nat. Struct. Biol.* **9,** 326–331
7. Jones, S., Smith, D. P., and Radford, S. E. (2003) *J. Mol. Biol.* **330,** 935–941
8. Esposito, G., Michelutti, R., Verdone, G., Viglino, P., Hernandez, H., Robinson, C. V., Amoresano, A., Dal Piaz, F., Monti, M., Pucci, P., Mangione, P., Stoppini, M., Merlini, G., Ferri, G., and Bellotti, V. (2000) *Protein Sci.* **9,** 831–845
9. Corazza, A., Pettirossi, F., Viglino, P., Verdone, G., Garcia, J., Dumy, P., Giorgetti, S., Mangione, P., Raimondi, S., Stoppini, M., Bellotti, V., and Esposito, G. (2004) *J. Biol. Chem.* **279,** 9176–9189
10. Chiti, F., Mangione, P., Andreola, A., Giorgetti, S., Stefani, M., Dobson, C. M., Bellotti, V., and Taddei, N. (2001) *J. Mol. Biol.* **307,** 379–391
11. Ivanova, M. I., Sawaya, M. R., Gingery, M., Attinger, A., and Eisenberg, D. (2004) *Proc. Natl. Acad. Sci. U. S. A.* **101,** 10584–10589
12. Trinh, C. H., Smith, D. P., Kalverda, A. P., Phillips, E. V., and Radford, S. E. (2002) *Proc. Natl. Acad. Sci. U. S. A.* **99,** 9771–9776
13. Verdone, G., Corazza, A., Viglino, P., Pettirossi, F., Giorgetti, S., Mangione, P., Andreola, A., Stoppini, M., Bellotti, V., and Esposito, G. (2002) *Protein Sci.* **11,** 487–499
14. Bjorkman, P. J., Saper, M. A., Samraoui, B., Bennett, W. S., Strominger, J. L., and Wiley, D. C. (1987) *Nature* **329,** 506–512
15. Floege, J., and Ketteler, M. (2001) *Kidney Int.* **59,** 164–171
16. Gejyo, F., Yamada, T., Odani, S., Nakagawa, Y., Arakawa, M., Kunitomo, T., Kataoka, H., Suzuki, M., Hirasawa, Y., Shirahama, T., Cohen, A. S., and Schmid, K. (1985) *Biochem. Biophys. Res. Commun.* **129,** 701–706
17. Hoshino, M., Kato, H., Hagihara, Y., Hasegawa, K., Naiki, H., and Goto, Y. (2002) *Nature Struct. Biol.* **9,** 332–336
18. Amzel, L. M., and Poljak, R. L. (1979) *Annu. Rev. Biochem.* **48,** 961–997
19. Tsunenaga, M., Goto, Y., Kawata, Y., and Hamaguchi, K. (1987) *Biochemistry* **26,** 6044–6051
20. Goto, Y., Ichimura, N., and Hamaguchi, K. (1988) *Biochemistry* **27,** 1670–1677
21. Chiba, T., Hagihara, Y., Higurashi, T., Hasegawa, K., Naiki, H., and Goto, Y. (2003) *J. Biol. Chem.* **278,** 47016–47024
22. Kozhukh, G. V., Hagihara, Y., Kawakami, T., Hasegawa, K., Naiki, H., and Goto, Y. (2002) *J. Biol. Chem.* **277,** 1310–1315
23. Kihara, M., Chatani, E., Sakai, M., Hasegawa, K., Naiki, H., and Goto, Y. (2005) *J. Biol. Chem.* **280,** 12012–12018
24. Ohhashi, Y., Kihara, M., Naiki, H., and Goto, Y. (2005) *J. Biol. Chem.* **280,** 32843–32848
25. Ban, T., Hoshino, M., Takahashi, S., Hamada, D., Hasegawa, K., Naiki, H., and Goto, Y. (2004) *J. Mol. Biol.* **344,** 757–767
26. McPherson, A. (1992) *J. Cryst. Growth* **122,** 161–167
27. Leslie, A. G. W. (1992) *Acta Crystallogr. Sect. D* **55,** 1696–1702
28. CCP4 Collaborative Computational Project, Number 4. (1994) *Acta Crystallogr. Sect. D* **50,** 760–763
29. Vagin, A., and Teplyakov, A. (1997) *J. Appl. Crystallogr.* **30,** 1022–1025
30. Jones, T. A., Zou, J. Y., Cowan, S. W., and Kjeldgaard, M. (1991) *Acta Crystallogr. Sect. A* **47,** 110–119
31. Murshudov, G. N., Vagin, A. A., and Dodson, E. J. (1997) *Acta Crystallogr. Sect. D* **53,** 240–255
32. Brunger, A. T. (1992) *Nature* **355,** 472–475
33. Laskowski, R. A., Rullmannn, J. A., MacArthur, M. W., Kaptein, R., and Thornton, J. M. (1996) *J. Biomol. NMR* **8,** 477–486
34. Yamaguchi, K., Takahashi, S., Kawai, T., Naiki, H., and Goto, Y. (2005) *J. Mol. Biol.* **352,** 952–960
35. Yamamoto, S., Hasegawa, K., Yamaguchi, I., Tsutsumi, S., Kardos, J., Goto, Y., Gejyo, F., and Naiki, H. (2004) *Biochemistry* **43,** 11075–11082
36. Katou, H., Kanno, T., Hoshino, M., Hagihara, Y., Tanaka, H., Kawai, T., Hasegawa, K., Naiki, H., and Goto, Y. (2002) *Protein Sci.* **11,** 2218–2229
37. Narimoto, T., Sakurai, K., Okamoto, A., Chatani, E., Hoshino, M., Hasegawa, K., Naiki, H., and Goto, Y. (2004) *FEBS Lett.* **576,** 313–319
38. Cowgill, R. W. (1970) *Biochim. Biophys. Acta* **207,** 556–559
39. Chatani, E., Kato, M., Kawai, T., Naiki, H., and Goto, Y. (2005) *J. Mol. Biol.* **352,** 941–951
40. Dzwolak, W., Smirnovas, V., Jansen, R., and Winter, R. (2004) *Protein Sci.* **13,** 1927–1932
41. Jones, E. M., and Surewicz, W. K. (2005) *Cell* **121,** 63–72
42. Tanaka, M., Chien, P., Yonekura, K., and Weissman, J. S. (2005) *Cell* **121,** 49–62
43. Koradi, R., Billeter, M., and Wüthrich, K. (1996) *J. Mol. Graph.* **14,** 51–55

Conformation of Amyloid Fibrils of β_2-Microglobulin Probed by Tryptophan Mutagenesis

Miho Kihara, Eri Chatani, Kentaro Iwata, Kaori Yamamoto, Takanori Matsuura, Atsushi Nakagawa, Hironobu Naiki and Yuji Goto

J. Biol. Chem. 2006, 281:31061-31069.
doi: 10.1074/jbc.M605358200 originally published online August 10, 2006

Supplemental Figures

CONFORMATION OF AMYLOID FIBRILS OF β_2-MICROGLOBULIN PROBED BY TRYPTOPHAN MUTAGENESIS*

Miho Kihara, Eri Chatani, Kentaro Iwata, Kaori Yamamoto, Takanori Matsuura, Atsushi Nakagawa, Hironobu Naiki, and Yuji Goto

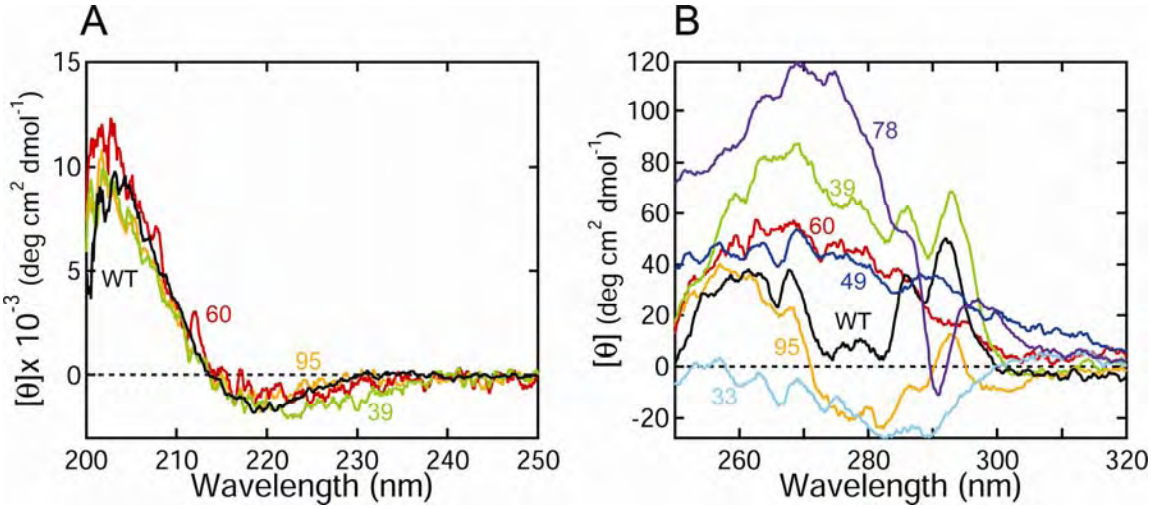

SUPPLEMENTAL FIGURE 1. CD spectra of wild-type and single Trp β2-ms at pH 8.0. (A) Far-UV CD spectra of wild-type (black), W60 (red), and W95 (orange) β2-ms. The spectra of other mutants indicated in (B) were superimposed on these spectra and are not shown for clarity. (B) Near-UV CD spectra. The spectra of wild-type and single Trp mutants are indicated with Trp residue numbers. CD spectra were measured at with a Jasco J-600 spectropolarimeter at 25 ˚C as described previously (1).

1. Chiba,T., Hagihara, Y., Higurashi, T., Hasegawa, K., Naiki, H. & Goto, Y. (2003) *J. Biol. Chem.* **278**, 47016-47024.

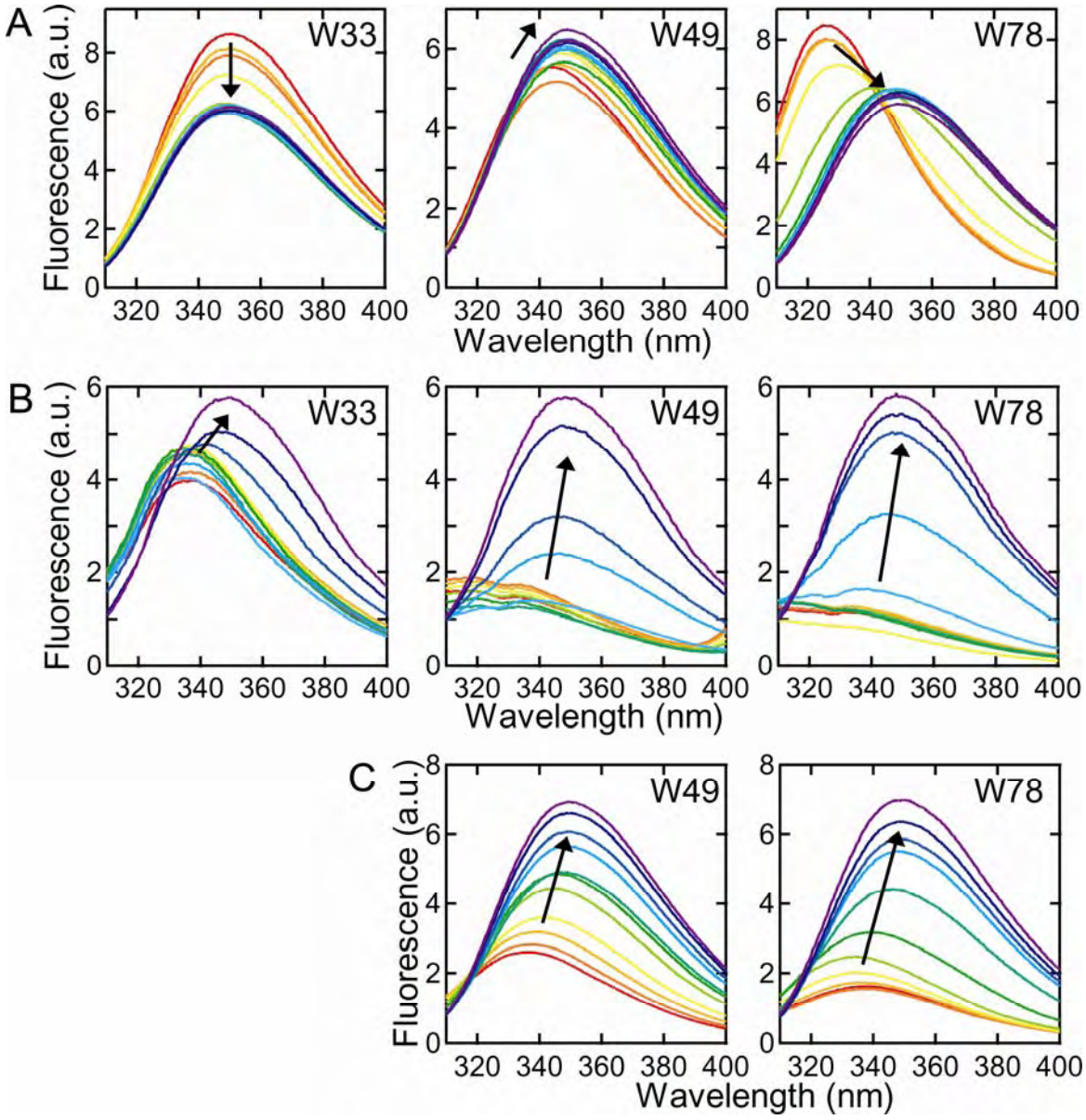

SUPPLEMENTAL FIGURE 2. Unfolding transitions of various single Trp β2-m mutants in the native states and amyloid fibrils. Unfolding transitions were monitored by Trp fluorescence spectrum of single Trp β2-m mutants (W33, W39, and W78) in the monomeric state at pH 8.0 (A) and in the amyloid fibrils at pH 2.5 (B) and pH 7.0 (C). (A, B) The concentration of Gdn-HCl increases from 0 M (red) to 5.5 M (purple) in steps of 0.5 M, as guided by an arrow. (C) The concentration of urea increases from 0 M (red) to 10.0 M (purple) in steps of 1.0 M, as guided by an arrow. The spectra of W33 were not obtained in the absence of enough amount of W33 fibrils at pH 7.0.

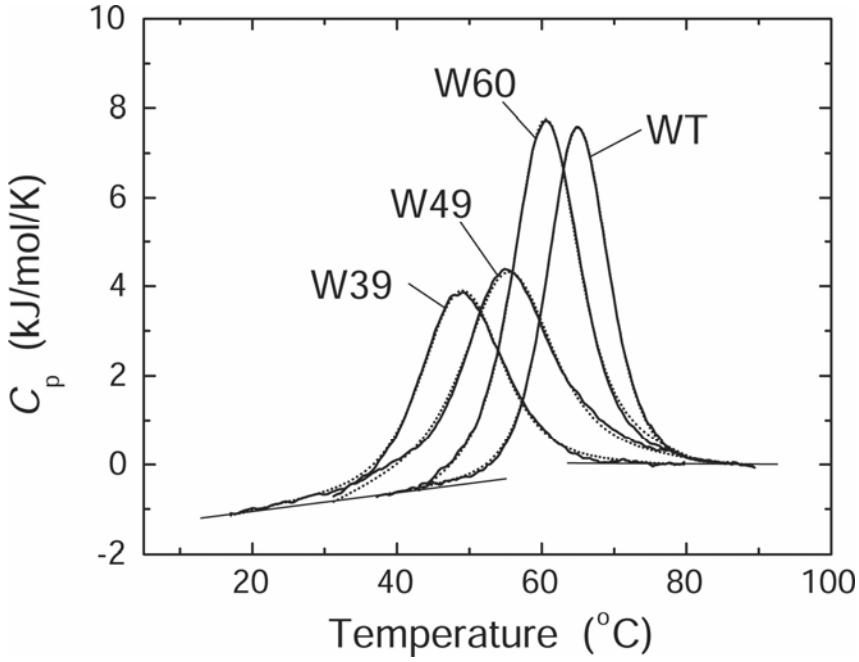

SUPPLEMENTAL FIGRURE 3. Calorimetric melting profile of single Trp β2-m mutants at pH 7.5. The dashed line represents a two-state fitting assuming the baselines indicated by solid lines. The T_m and ΔH at T_m are 65.1 ˚C and 344. kJ/mol for the wild type, 48.8 ˚C and 227 kJ/mol for W39, 55.6 ˚C and 222 kJ/mol for W49, and 60.5 ˚C and 303 kJ/mol for W60, respectively. Calorimetric measurements were performed at the protein concentration of 0.3 mg/ml in 50 mM Na phosphate buffer (pH 7.0) containing 100 mM NaCl as described previously (1).

1. Kardos, J., Yamamoto, K., Hasegawa, K., Naiki, H., and Goto, Y. (2004) *J. Biol. Chem.* **279**, 55308-55314.